Report No. C-SAFE-CD-IR-04-003

MPM VALIDATION: SPHERE-CYLINDER IMPACT: MEDIUM RESOLUTION SIMULATIONS

B. Banerjee
Department of Mechanical Engineering, University of Utah, Salt Lake City, UT 84112, USA
August 12, 2004

ABSTRACT

In a previous report we compared the experimental and the computed axial velocity and axial strain from a low spatial resolution study of the impact of an aluminum sphere on an aluminum plate supported by a hollow aluminum cylinder. We report results from a higher resolution study of the same problem using input parameters that conserve both momentum and energy quite accurately. The simulations show a slower wave speed than the experiments which suggests that the elastic moduli and density of the material used in the experiments may be different from those used in the simulations. The simulated free surface velocity also differs from the experimental data. Further study is required to determine the cause of these differences.

1 INTRODUCTION

The validation experiments described in this report simulate the impact of a 6061-T6 aluminum sphere against a plate attached to a hollow cylinder of the same material (Chhabildas et al. [1]). We compare the free surface velocity histories for four experiments - L1, L3, L5, and L6 and the axial strain histories for three experiments - L3, L5, and L6. Figures 1(a), 1(b), 1(c), and 1(d) show the geometries for L1, L3, L5, and L6, respectively.

The set of input parameters that best conserves energy and momentum has been described before (Banerjee [2]). The approach used to determine the axial velocities and strains from the simulations has been described in detail in our previous report (Banerjee [3]). The simulations shown in this report were performed using 20 particles along the thickness of the front plate and 60 particles along the radius. For the cylinder, we used a resolution of 100 particles along the axial direction and 6 particles The background mesh had a resolution of $100 \times 40 \times 40$. Each of the runs took around 19 hours of wall time using 16 processors. The input file for experiment L3 is shown in Appendix I.

The energy and momentum plots for experiment L1 are shown in Figure 2(a) and (b). Those for experiments L3 (with and without damping) are shown in Figure 2(c),(d), (e), and (f). Energy and momentum plots for L5 and L6 are shown in Figures 3, and 4, respectively. The plots show that momentum is conserved almost exactly for all the cases. Energy is conserved extremely well for all the undamped simulations. The expected energy dissipation in the damped simulation of experiment L3 can also be observed from Figure 2(e).

Section 2 shows the results for experiment L1. Two sets of particles at depths of 1 mm and 1.5 mm from the free surface, respectively, have been probed for their velocity history. These velocities are compared with experimental data for L1. Results for experiment L3 are discussed in Section 3. The damped and undamped simulations are compared and the free-surface velocity histories are compared and well as the axial strains at gages S1, S2, S4, S5, and S6. Results for experiment L5 are discussed in Section 4. These include the free-surface velocity and the axial strains at all the strain gages without damping. Results for experiment L6 are discussed in Section 5. The velocity history

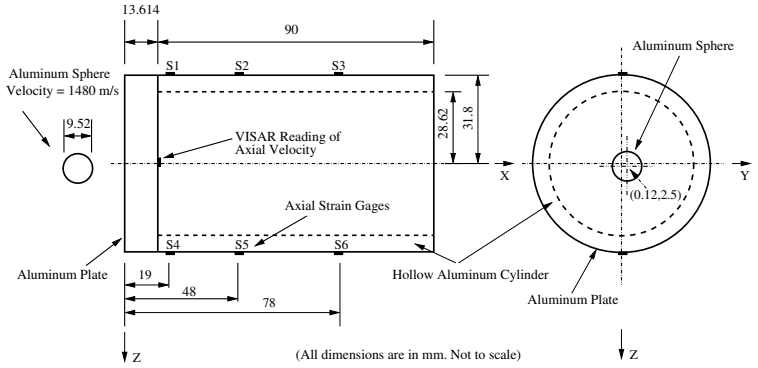

(a) Initial geometry of experiment L1.

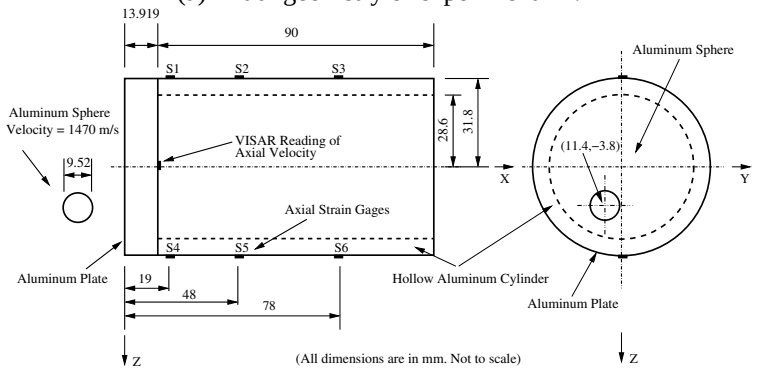

(b) Initial geometry of experiment L3.

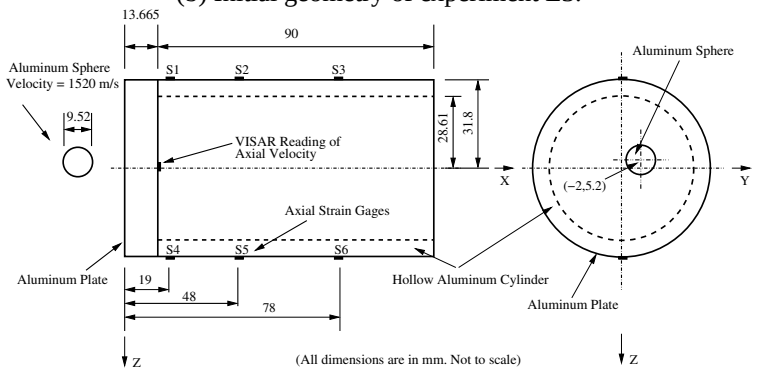

(c) Initial geometry of experiment L5.

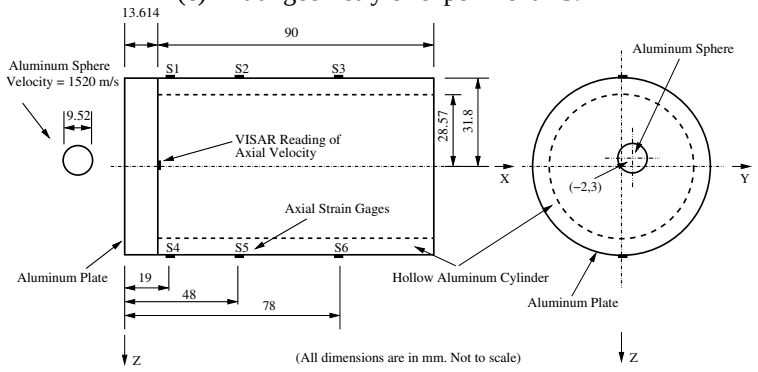

(d) Initial geometry of experiment L6.

Figure 1: Initial geometry of impact experiments.

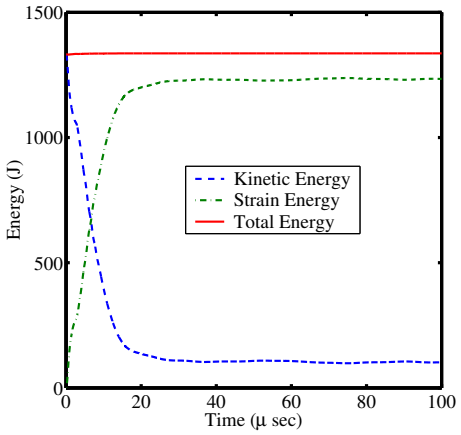

(a) Energy evolution for experiment L1.

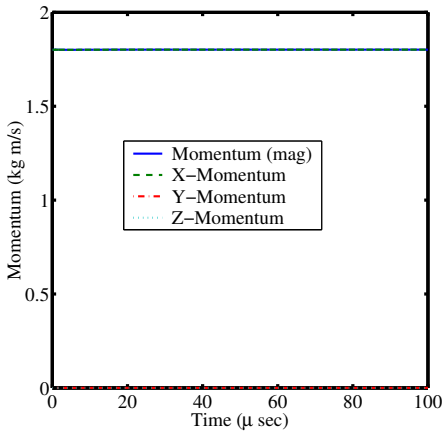

(b) Momentum evolution for experiment L1.

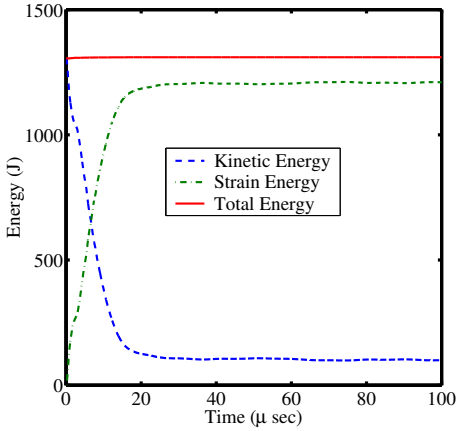

(c) Energy evolution for experiment L3 (without damping).

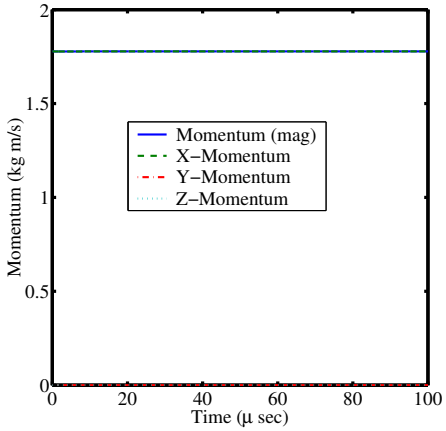

(d) Momentum evolution for experiment L3 (without damping).

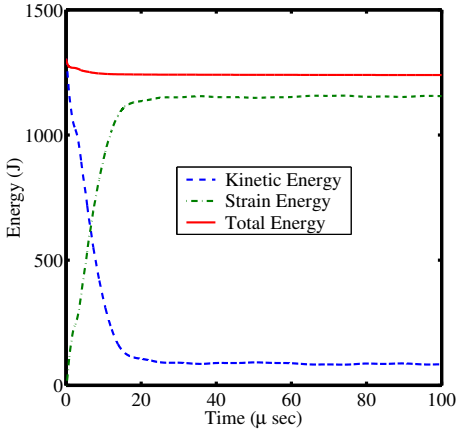

(e) Energy evolution for experiment L3 (with damping).

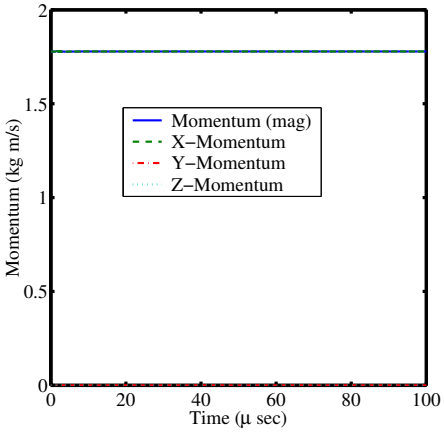

(f) Momentum evolution for experiment L3 (with damping).

Figure 2: Energy and momentum evolution for experiments L1 and L3.

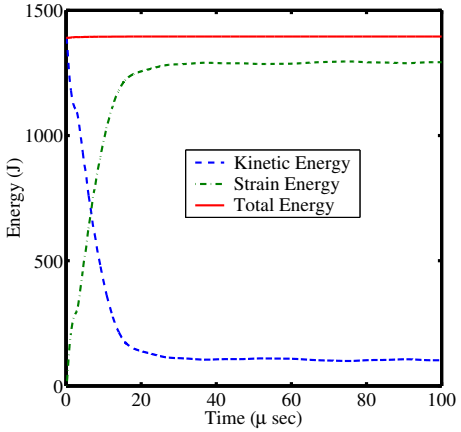

(a) Energy evolution for experiment L5.

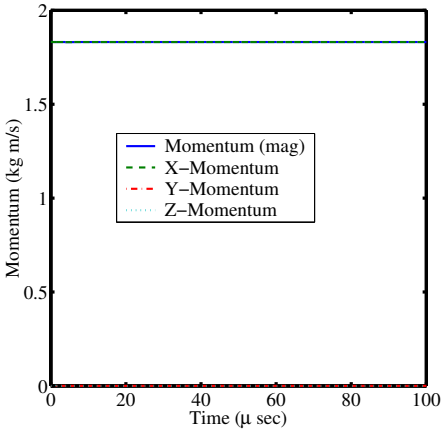

(b) Momentum evolution for experiment L5.

Figure 3: Energy and momentum evolution for experiment L5.

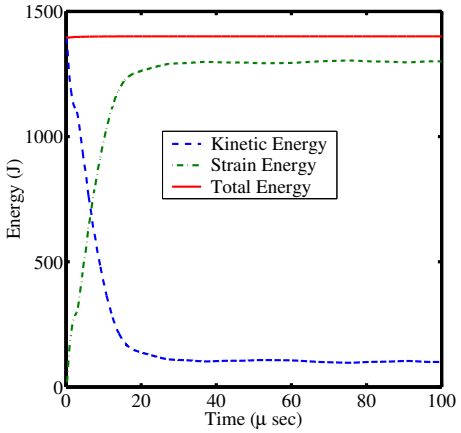

(a) Energy evolution for experiment L6.

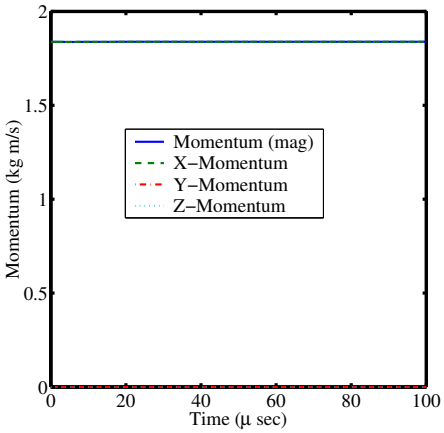

(b) Momentum evolution for experiment L6.

Figure 4: Energy and momentum evolution for experiment L6.

at the free surface and the strains at gage S2 are compared with experimental data. Conclusions and future work are discussed in Section 6.

2 EXPERIMENT L1

The particle identifiers used for velocity data extraction for the simulations are shown in Figure 5(a). These particles are located at a depth of approximately $1\ mm$ from the free surface of the plate. As there are no particles at the exact location of the VISAR readings, we have chosen to average the velocity over particles located along each of the paths shown in red in the figure. Figure 5(b) shows plots of the simulated and experimental free surface velocity for experiment L1.

The initial time of arrival appears not to match the experimental data. This is probably due to the interval at which we sample the velocity. A run with a higher rate of sampling is currently being

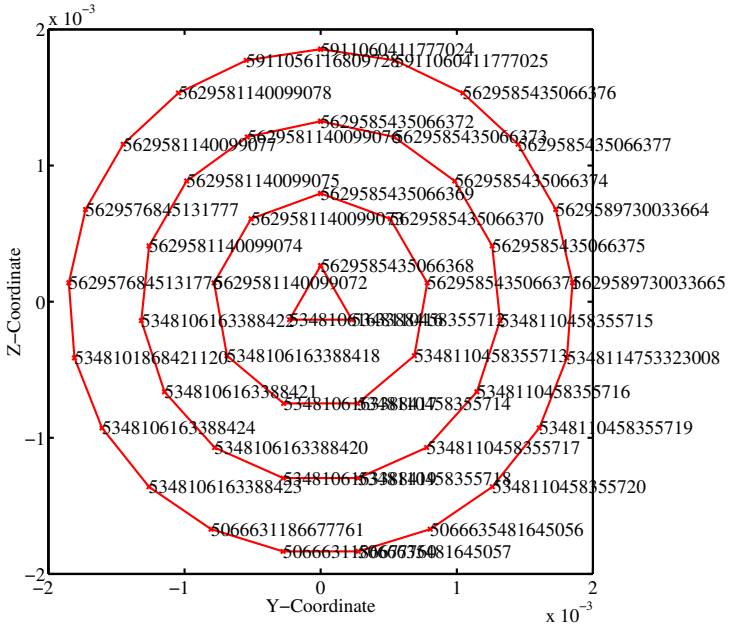

(a)Particle tags used for free surface velocity data extraction.

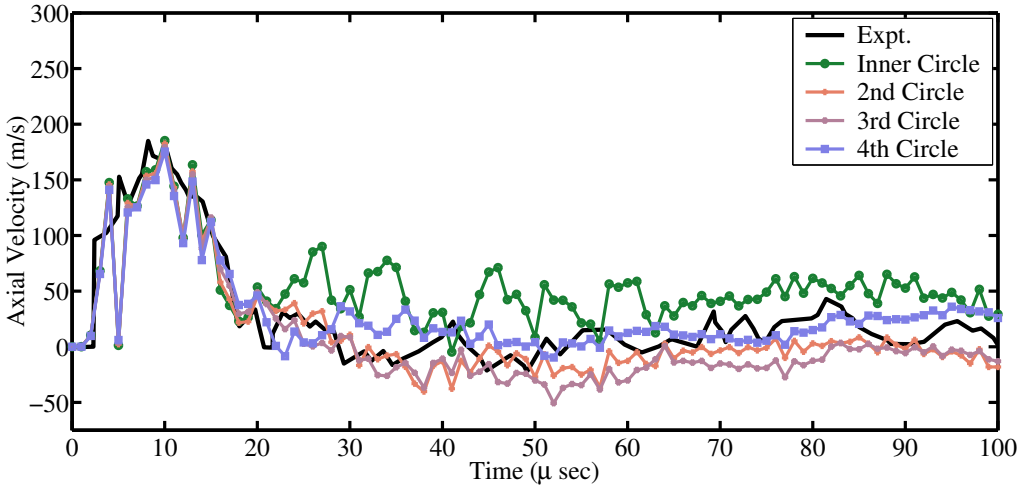

(b)Velocity history for experiment L1.

Figure 5: Particle tags and average velocity history for experiment L1.

performed. After the initial peak velocity is reached, there is an immediate sharp drop off to almost zero velocity. This drop reduces slightly if artificial damping is used and is probably the result of the shock not being resolved sufficiently.

Though the simulated free-surface velocity shows some ringing up to 20 μs, it matches the experimental data quite well on average. Beyond that time, the particles in the inner circle show much higher velocities than the experimental data. Particles in the second circle match the experimental data most closely (in a least squares sense) for the first 50 μs while particles in the fourth circle provide the best match beyond that time.

We wanted to check if the large initial fluctuation the the free-surface velocity was due to the location of the particles. With that in mind, we also looked at the velocities at a depth of $1.5\ mm$ from the surface. The particle tags for these particles are shown in Figure 6(a). Figure 6(b) shows plots of the simulated and experimental free surface velocity for experiment L1 for particles at a depth of 1.5 mm from the surface.

The data clearly show that much higher velocities are observed on the plane at a depth of 1.5 mm from the surface. Chhabildas et al. [1] concluded that the yield strength of 6061-T6 Aluminum is 400 MPa based on velocities at a similar depth which generated a plot similar to Figure 6(b). We feel that such a conclusion is not justified because the magnitude of the free-surface velocities is captured very well with a the initial yield strength pf 324 MPa used by the Johnson-Cook model as can be seen in Figure 5.

3 EXPERIMENT L3

As suggested in the previous report (Banerjee [3]) we ran simulations with and without damping for experiment L3. Figure 7(a) shows plots of the simulated and experimental free surface velocity for experiment L3 without damping. Figure 7(b) shows the velocities with damping. Experimental velocity data are available only up to 16 μs for this case.

The initial peak velocities match the experimental data very well. However, the high velocities remain for around 7-10 μs longer than is seen in the experimental data. Large fluctuations in the initial velocities are damped out in Figure 7(b), but the apparently delayed response of the simulated velocities remains. There can be a number of causes for this difference which should be explored further.

The strain histories with and without damping are shown in Figures 8, 9, 10, 11, and 12. The simulated strains shown in the figures represent the average over 28-40 particles depending on the location of the strain gage. The top plot in each figure shows the strain without damping while the bottom plot shows the strain with artificial damping turned on. It is clear from the plots that artificial damping affects only the high frequencies in the strain history.

The strain at gage S1 (Figure 8) matches the experimental data quite well initially but tends to drift with time, though the trends remain similar. This suggests that the stress waves is traveling more slowly in the simulations than in the experiments. The amplitude of the wave is also lower with time. We believe that the boundary conditions at the end of the cylinder may be slowing down the reflected wave and causing this anomaly. A one-dimensional wave propagation problem should be used to verify the accuracy of the MPM code in this regard.

Similar trends are observed for gage S2 (Figure 9. The initial trend matches the experimental data. However, with time the compute stress wave appears to lag behind the experimental data and the peak amplitude of the strain also seems to be lower.

Gage S4 is closest to the point of impact in experiment L3. This is reflected my the high compressive strains shown in Figure 10. The initial computed strains match the experimental data extremely well. However, once again we observe a lag as time increases though the trend of the

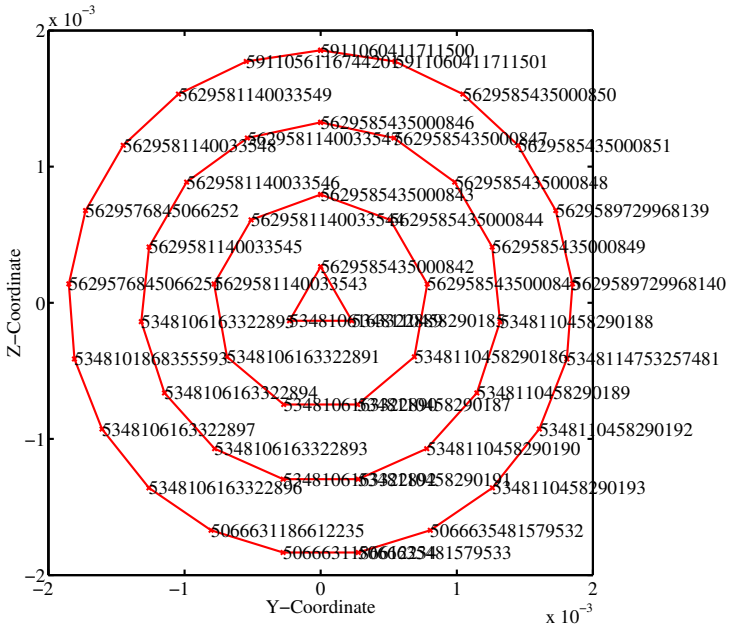

(a) Particle tags used for free surface velocity data extraction at a depth of 1.5 mm from the surface.

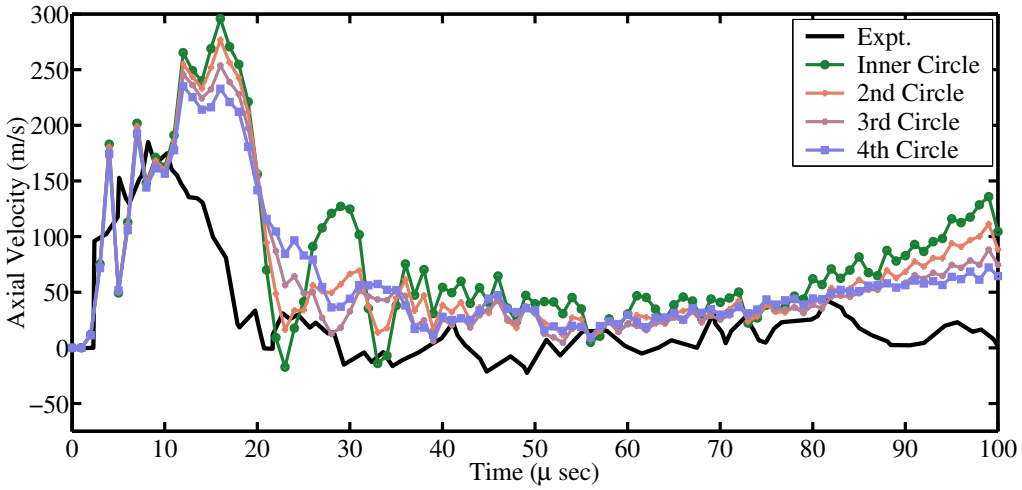

(b) Velocity history for experiment L1 for particles at a depth of 1.5 mm from the surface.

Figure 6: Particle tags and average velocity history for experiment L1 at a depth of 1.5 mm from the surface.

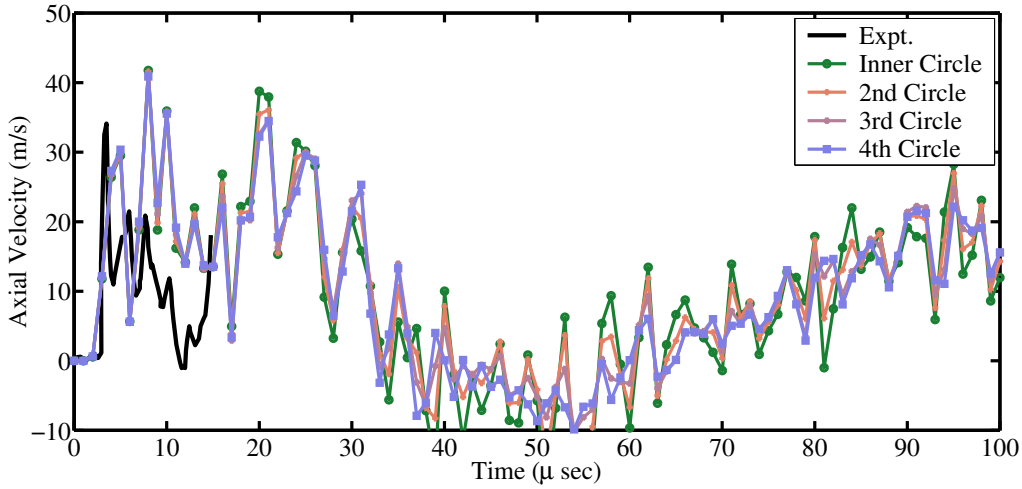

(a) Without damping.

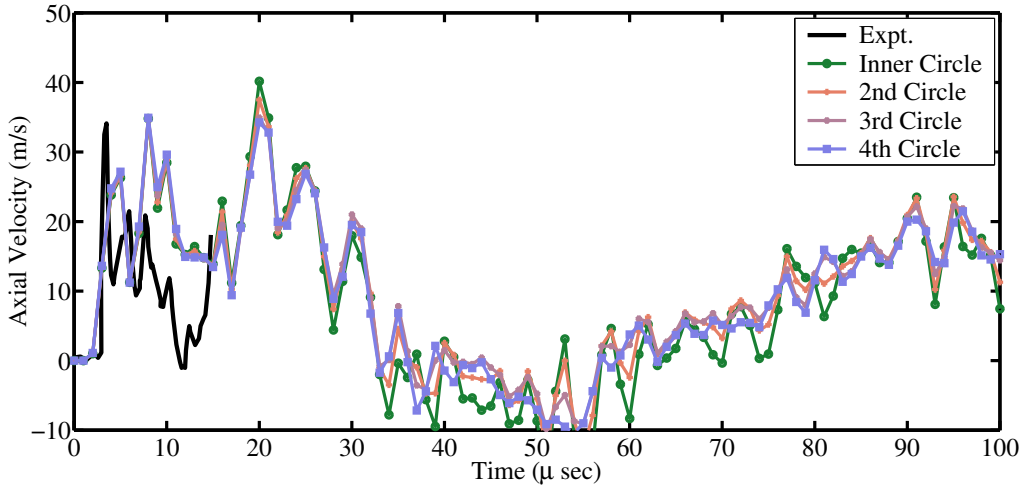

(b) With damping.

Figure 7: Velocity history for experiment L3.

strain history matches the experimental data quite well.

The simulated strains match the experimental strains at L5 and L6 quite well at initial times but the tendency to drift at later times is similar to that observed for the other strain gages. This can be seen in Figures 11 and 12. Perhaps a higher resolution study is required to determine if the mesh resolution plays any part in the wave propagation velocity in MPM. This conjecture is based on the observation that the lower resolution studies in our previous report (Banerjee [3]) showed an even slower apparent wave speed. The size of the computational box should also be increased in the direction of impact so that the cylinder does not hit the walls of the computational domain and

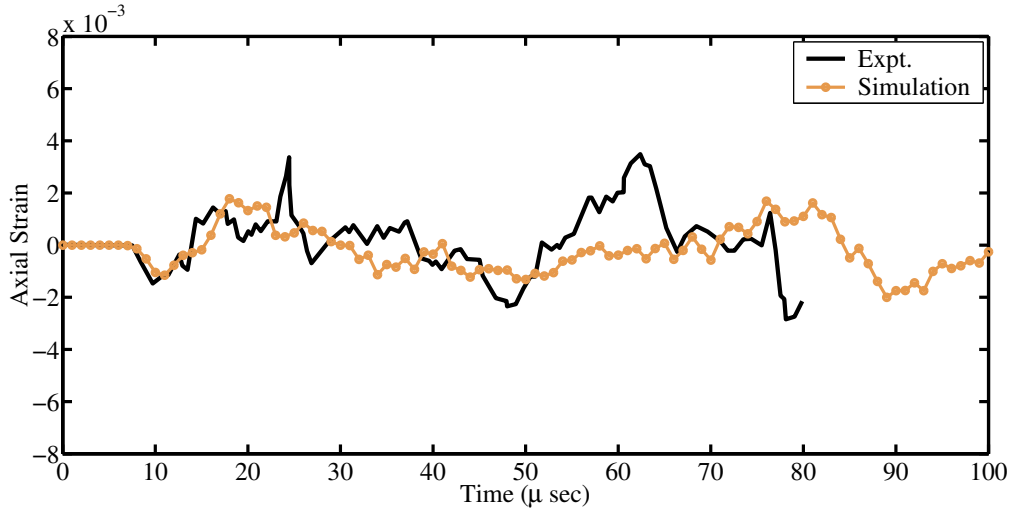

(a) Gage S1 - without damping.

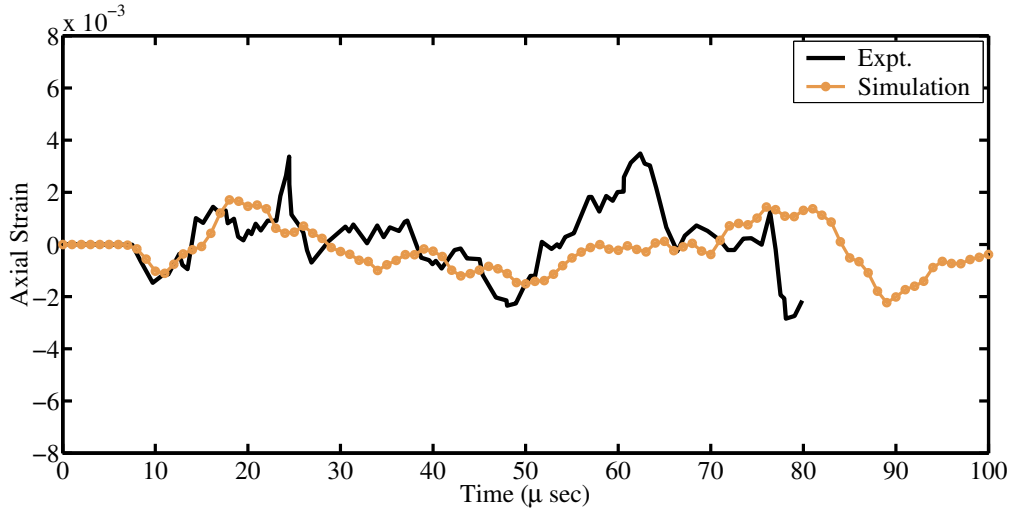

(b) Gage S1 - with damping.

Figure 8: Strain histories for experiment L3: gage S1.

reflect waves in an unplanned manner.

4 EXPERIMENT L5

Figure 13 shows the velocity history for experiment L5. In this case, the experimental data are available up to around 12 μs. The computed peak velocities are around 120 m/s while the experimental peak is approximately 170 m/s. This difference could be due to variability in material properties of the aluminum plate.

The strain histories for experiment L5 are shown in Figures 14, 15 and 16. Since the aluminum cylinder is the same between experiments and undergoes only elastic deformations, we expect to see

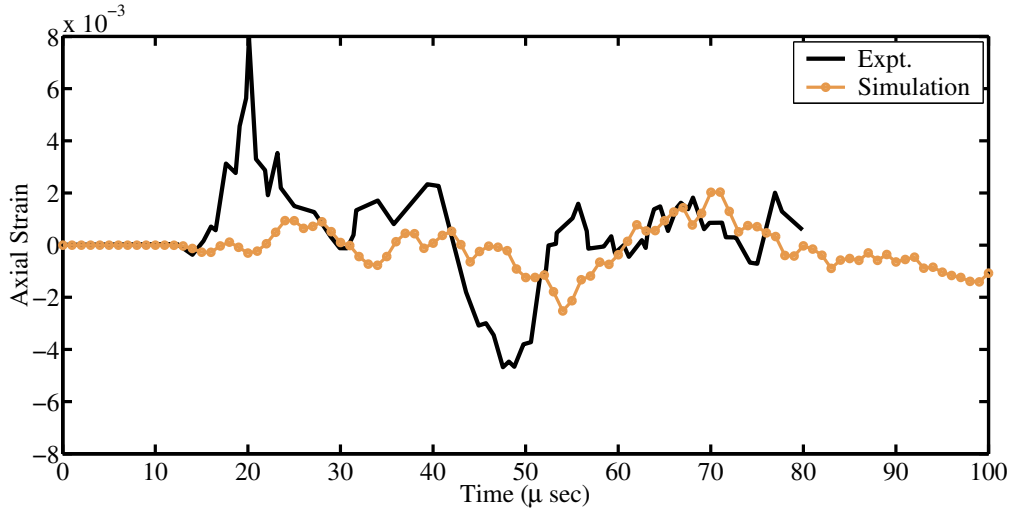

(a) Gage S2 - without damping.

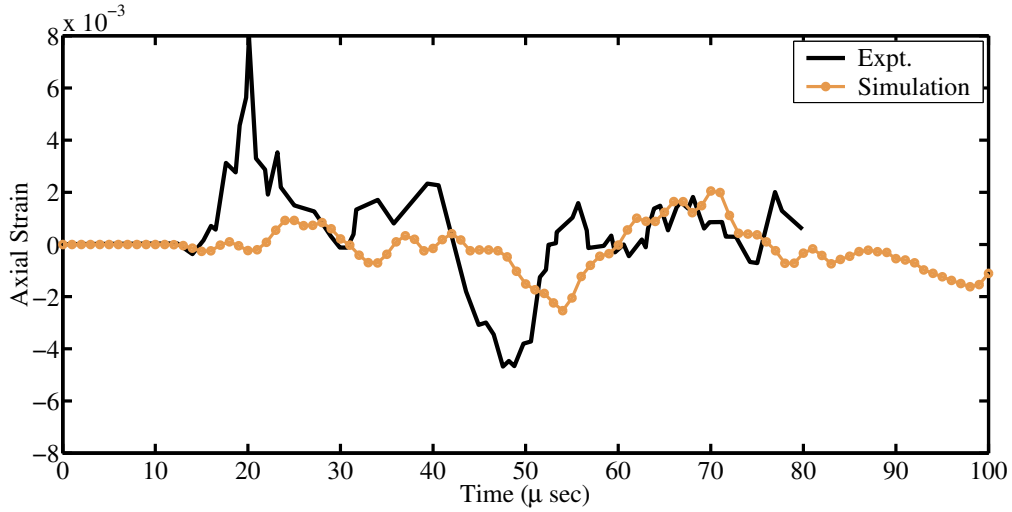

(b) Gage S2 - with damping.

Figure 9: Strain histories for experiment L3: gage S2.

uniform behavior between experiments. This conjecture is borne out by the strain gage results for experiment L5.

As observed before, the strain history of gages S1 and S2 show good agreement with experimental data at initial times. However, with time the computed stress wave again appears to lag behind the experimental data since the trends are similar but separated by 5-7 μs. If we consider a one-dimensional pressure wave, this lag implies a wave velocity that is 1-2% smaller than the actual wave velocity of the material. This should be reflected in the initial time for the stress wave to reach the strain gage. However, the arrival time is computed quite accurately. It is therefore unlikely that the lag is due to incorrect bulk and shear moduli. The more likely reason is that the

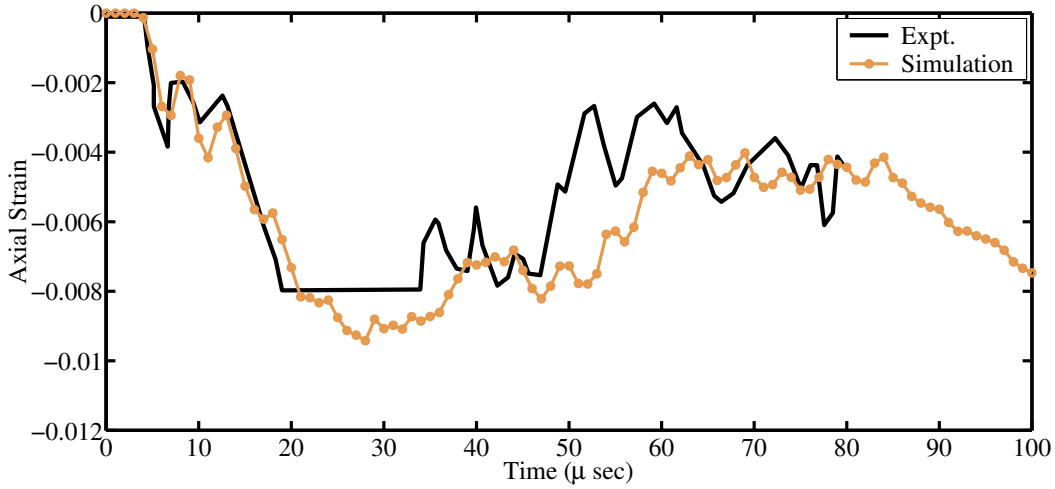

(a) Gage S4 - without damping.

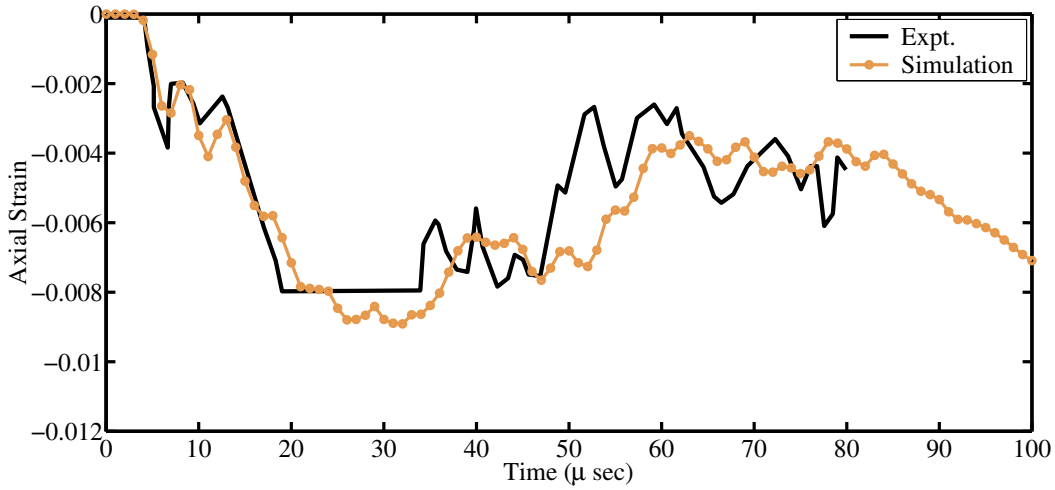

(b) Gage S4 - with damping.

Figure 10: Strain histories for experiment L3: gage S4.

stress wave reflects off the back end of the front plate in the actual experiment whereas in our MPM calculations there is no interface between the cylinder and the plate. Hence, in our computations the wave reflects of the impact surface and hence reaches the strain gage later in time. This possibility is further strengthened by the fact that the lag occurs later in time for strain gages further from the impact plane. We suggest that an interface be introduced between the cylinder and the plate and the simulations rerun.

Strain gage S3 shows a slight offset from the experimental data from the time the stress wave arrives at the gage (as shown in Figure 15(a)). However, the experimental data shows significant fluctuations beyond that points which are not reflected in the computations. This could be due to incorrect digitization of the experimental strain plots. The plots shown in Chhabildas et al. [1] can

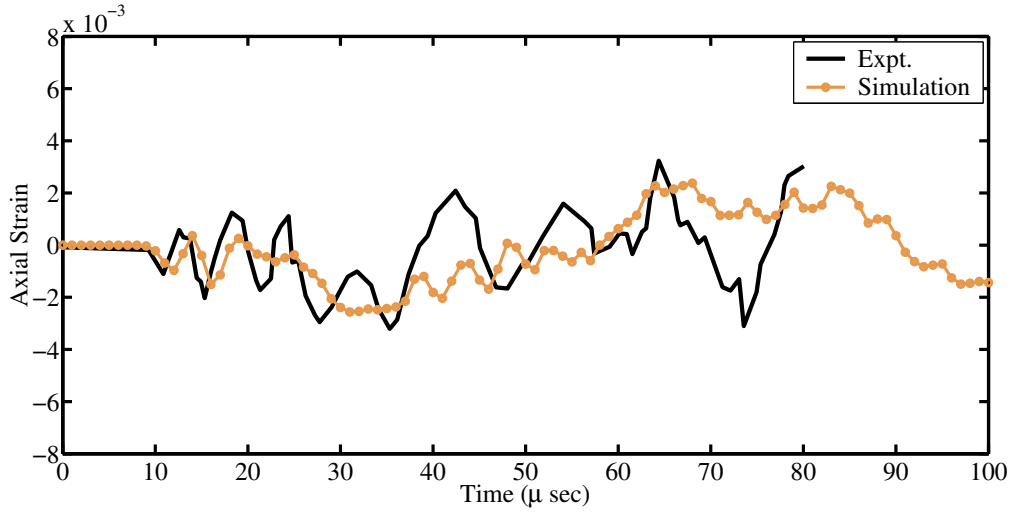

(a) Gage S5 - without damping.

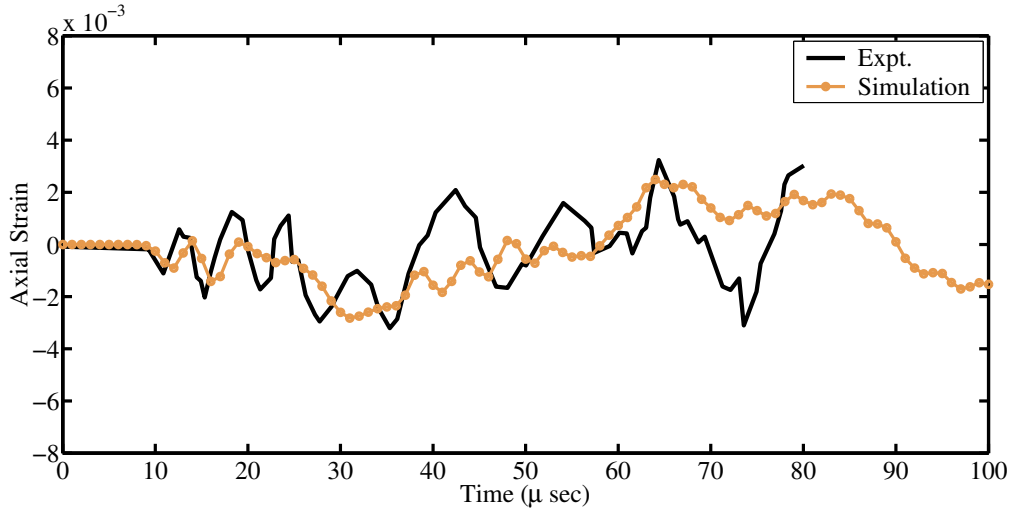

(b) Gage S5 - with damping.

Figure 11: Strain histories for experiment L3: gages S5.

not be clearly distinguished from each other.

The initial strains in gage S4 match the experimental data well up to around 30 μs (see Figure 15(b)). The lag in the computed strains is clear beyond that point and could be due to the reasons discussed earlier.

Initial arrival times for gages S5 and S6 match the experimental data well but exhibit the same lags as in the other cases and lower strain amplitudes than the experimental data. These can be seen in Figures 16(a) and (b).

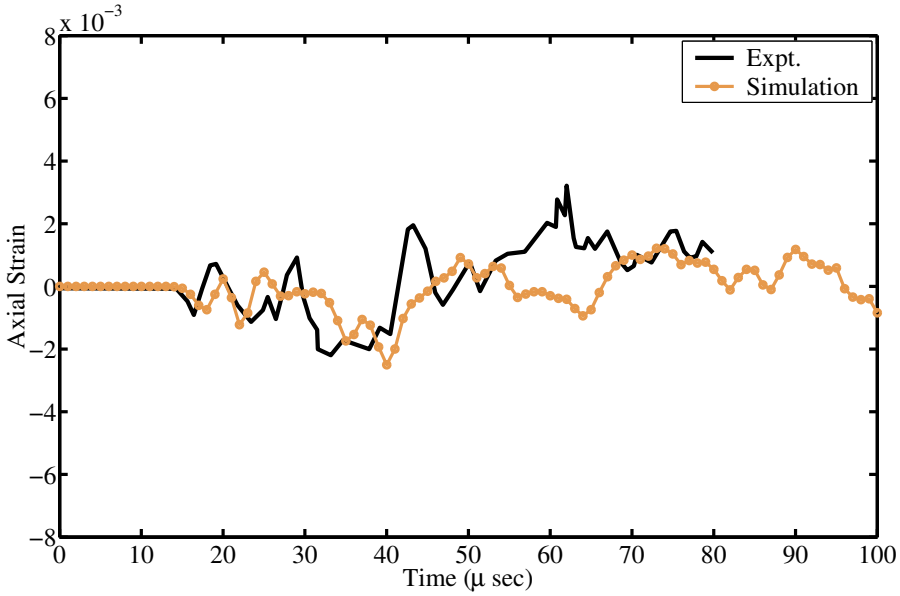

(a) Gage S6 - without damping.

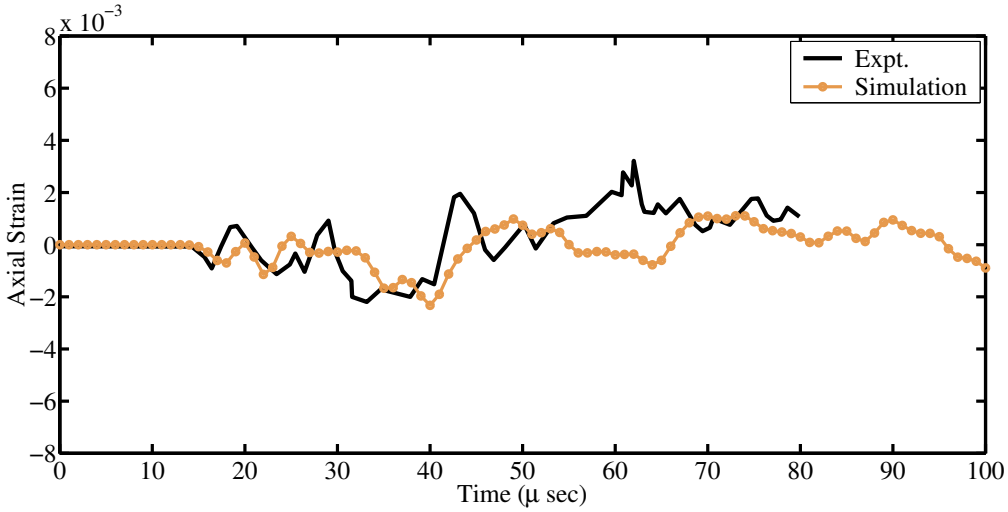

(b) Gage S6 - with damping.

Figure 12: Strain histories for experiment L3: gage S6.

5 EXPERIMENT L6

Figure 17(a) shows the velocity history for experiment L6. The experimental data are available only up to 18 μs. Barring initial fluctuations, the experimental velocities are matched well by the simulations. However, the peaks are slightly offset and the computed peak value is lower than the experimental. The strain history for gage S2 in experiment L6 is shown in Figure 17(b). As discussed before, the the initial strains are matched well by the simulations but a drift is observed

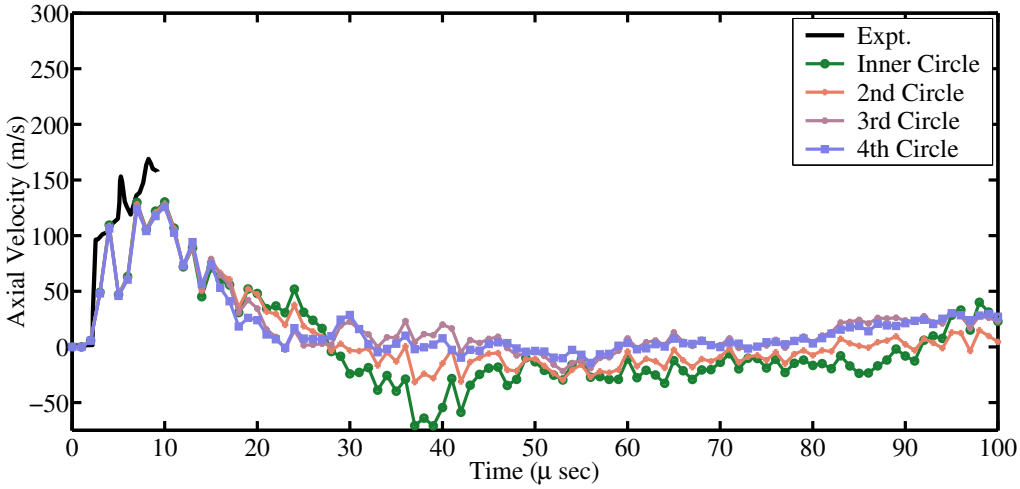

Figure 13: Velocity history for experiment L5.

with increasing time.

6 CONCLUSION

The initial arrival times are matched well by the simulations. With time, however, a drift in the computed values is observed relative to the experiments. In other words, the computed wave speed appears to decrease with time. One cause of this anomaly could be the use of a single material to model the front plate and the cylinder leading to reflections from the impact plane instead of the back of the plate. Another reason could be the size of the domain. It is possible that the domain in not large enough to accommodate the axial movement of the cylinder after impact. Other reasons could be the resolution of the grid. The sampling rate could be the reason some of the high amplitude values are not being plotted and the cause of the apparent early arrival of the stress wave at the free surface.

ACKNOWLEDGMENTS

This work was supported by the the U.S. Department of Energy through the Center for the Simulation of Accidental Fires and Explosions, under grant W-7405-ENG-48.

REFERENCES

[1] Chhabildas, L. C., Konrad, C. H., Mosher, D. A., Reinhart, W. D., Duggins, B. D., Trucano, T. G., Summers, R. M., and Peery, J. S. A methodology to validated 3D arbitrary Lagrangian Eulerian codes with applications to ALEGRA. *Int. J. Impact Engrg.*, 23:101–112, 1998.

[2] Banerjee, B. MPM validation: Sphere-cylinder impact tests: Energy balance. Technical Report C-SAFE-CD-IR-04-001, Center for the Simulation of Accidental Fires and Explosions, University of Utah, USA, 2004.

[3] Banerjee, B. MPM validation: Sphere-cylinder impact: Low resolution simulations. Technical Report C-SAFE-CD-IR-04-002, Center for the Simulation of Accidental Fires and Explosions, University of Utah, USA, 2004.

APPENDIX I. INPUT FILE : EXPERIMENT L3

```
<?xml version='1.0' encoding='ISO-8859-1' ?>
<!-- @version: -->
<Uintah_specification>

<!-- 6061 T6 Al Sphere impacting 6061 T6 Al Cylinder,
     Hypoelastic stress update,
     Johnson Cook Plasticity Model, Johnson Cook Damage Model,
     Default Hypoelastic Equation of State -->

   <Meta>
     <title>Sphere Impacting Cylinder</title>
   </Meta>

   <Time>
     <maxTime>      100.0e-6     </maxTime>
     <initTime>       0.0     </initTime>
     <delt_min>       0.0     </delt_min>
     <delt_max>       1e-5    </delt_max>
     <delt_init>      1e-7    </delt_init>
     <timestep_multiplier>0.1     </timestep_multiplier>
   </Time>

   <DataArchiver>
     <filebase>impactAlSphCylSmEroJCL3Sml.uda</filebase>
     <outputInterval> 1.0e-6 </outputInterval>
     <compression>gzip</compression>
     <outputDoubleAsFloat/>
     <save label = "p.particleID"/>
     <save label = "p.x"/>
     <save label = "p.stress"/>
     <save label = "p.velocity"/>
     <save label = "p.deformationMeasure"/>
     <save label = "p.localized"/>
     <save label = "AccStrainEnergy"/>
     <save label = "KineticEnergy"/>
     <save label = "ThermalEnergy"/>
     <save label = "CenterOfMassVelocity"/>
     <checkpoint cycle = "2" timestepInterval = "100"/>
   </DataArchiver>

   <MPM>
     <time_integrator>explicit</time_integrator>
     <nodes8or27> 27 </nodes8or27>
     <minimum_particle_mass> 1.0e-8</minimum_particle_mass>
     <maximum_particle_velocity> 1.0e8</maximum_particle_velocity>
     <artificial_damping_coeff> 0.0 </artificial_damping_coeff>
     <artificial_viscosity> false </artificial_viscosity>
     <artificial_viscosity_coeff1> 0.07 </artificial_viscosity_coeff1>
     <artificial_viscosity_coeff2> 1.6 </artificial_viscosity_coeff2>
     <accumulate_strain_energy> true </accumulate_strain_energy>
     <turn_on_adiabatic_heating> false </turn_on_adiabatic_heating>
     <use_load_curves> false </use_load_curves>
     <create_new_particles> true </create_new_particles>
     <erosion algorithm = "KeepStress"/>
   </MPM>

   <PhysicalConstants>
     <gravity>      [0,0,0]   </gravity>
```

```
  <reference_pressure> 101325.0  </reference_pressure>
</PhysicalConstants>

<MaterialProperties>
  <MPM>
    <material>
      <density>2700.0</density>
      <toughness>29.e6</toughness>
      <thermal_conductivity>166.9</thermal_conductivity>
      <specific_heat>896.0</specific_heat>
      <room_temp>294.0</room_temp>
      <melt_temp>925.0</melt_temp>
      <constitutive_model type = "elastic_plastic">
        <tolerance>1.0e-15</tolerance>
        <useModifiedEOS> true </useModifiedEOS>
        <evolve_porosity>false</evolve_porosity>
        <evolve_damage>true</evolve_damage>
        <compute_specific_heat>false</compute_specific_heat>
        <do_melting> true </do_melting>
        <check_TEPLA_failure_criterion>true</check_TEPLA_failure_criterion>
        <shear_modulus>26.0e9</shear_modulus>
        <bulk_modulus>66.4e9</bulk_modulus>
        <equation_of_state type = "default_hypo">
        </equation_of_state>
        <plasticity_model type = "johnson_cook">
          <A>324.0e6</A>
          <B>114.0e6</B>
          <C>0.002</C>
          <n>0.42</n>
          <m>1.34</m>
        </plasticity_model>
        <yield_condition type = "vonMises">
        </yield_condition>
        <stability_check type = "drucker_becker">
        </stability_check>
        <damage_model type = "johnson_cook">
          <D1>-0.77</D1>
          <D2>1.45</D2>
          <D3>-0.47</D3>
          <D4>0.0</D4>
          <D5>1.60</D5>
        </damage_model>
      </constitutive_model>
      <geom_object>
        <sphere label = "sphere">
          <origin>[9.75e-3, -3.8e-3, 11.4e-3]</origin>
          <radius> 4.75e-3 </radius>
        </sphere>
        <res>[2,2,2]</res>
        <velocity>[1470.0,0.0,0.0]</velocity>
        <temperature>294</temperature>
      </geom_object>
    </material>
    <material>
      <density>2700.0</density>
      <toughness>29.e6</toughness>
      <thermal_conductivity>166.9</thermal_conductivity>
      <specific_heat>896.0</specific_heat>
      <room_temp>294.0</room_temp>
```

```
  <melt_temp>925.0</melt_temp>
  <constitutive_model type = "elastic_plastic">
    <tolerance>1.0e-15</tolerance>
    <useModifiedEOS> true </useModifiedEOS>
    <evolve_porosity>false</evolve_porosity>
    <evolve_damage>true</evolve_damage>
    <compute_specific_heat>false</compute_specific_heat>
    <do_melting> true </do_melting>
    <check_TEPLA_failure_criterion>true</check_TEPLA_failure_criterion>
    <shear_modulus>26.0e9</shear_modulus>
    <bulk_modulus>66.4e9</bulk_modulus>
    <equation_of_state type = "default_hypo">
    </equation_of_state>
    <plasticity_model type = "johnson_cook">
      <A>324.0e6</A>
      <B>114.0e6</B>
      <C>0.002</C>
      <n>0.42</n>
      <m>1.34</m>
    </plasticity_model>
    <yield_condition type = "vonMises">
    </yield_condition>
    <stability_check type = "drucker_becker">
    </stability_check>
    <damage_model type = "johnson_cook">
      <D1>-0.77</D1>
      <D2>1.45</D2>
      <D3>-0.47</D3>
      <D4>0.0</D4>
      <D5>1.60</D5>
    </damage_model>
  </constitutive_model>
  <geom_object>
    <smoothcyl label = "end plate">
      <bottom>     [15.0e-3, 0.0, 0.0] </bottom>
      <top>        [28.919e-3, 0.0, 0.0] </top>
      <radius>     31.8e-3 </radius>
      <num_axial>  20 </num_axial>
      <num_radial> 60 </num_radial>
    </smoothcyl>
    <res>[2,2,2]</res>
    <velocity>[0.0,0.0,0.0]</velocity>
    <temperature>294</temperature>
  </geom_object>
  <geom_object>
    <smoothcyl label = "hollow cylinder">
      <bottom>     [28.919e-3, 0.0, 0.0] </bottom>
      <top>        [119.0e-3, 0.0, 0.0] </top>
      <radius>     31.8e-3 </radius>
      <thickness>  3.20e-3 </thickness>
      <num_axial>  100 </num_axial>
      <num_radial> 60 </num_radial>
    </smoothcyl>
    <res>[2,2,2]</res>
    <velocity>[0.0,0.0,0.0]</velocity>
    <temperature>294</temperature>
  </geom_object>
</material>
<contact>
```

```
        <type>single_velocity</type>
        <mu>0.0001</mu>
        <vel_fields>[0,0,0]</vel_fields>
      </contact>
    </MPM>
  </MaterialProperties>

  <PhysicalBC>
    <MPM>
    </MPM>
  </PhysicalBC>

  <Grid>
    <Level>
      <Box label = "1">
        <lower>[0.0, -33.0e-3,-33.0e-3]</lower>
        <upper>[119.0e-3, 33.0e-3, 33.0e-3]</upper>
        <patches>[16,1,1]</patches>
        <extraCells>[1,1,1]</extraCells>
        <resolution>[100, 40, 40]</resolution>
      </Box>
    </Level>
    <BoundaryConditions>
      <Face side = "x-">
        <BCType id = "0" label = "Symmetric" var = "symmetry">
        </BCType>
      </Face>
      <Face side = "x+">
        <BCType id = "0" label = "Symmetric" var = "symmetry">
        </BCType>
      </Face>
      <Face side = "y-">
        <BCType id = "0" label = "Symmetric" var = "symmetry">
        </BCType>
      </Face>
      <Face side = "y+">
        <BCType id = "0" label = "Symmetric" var = "symmetry">
        </BCType>
      </Face>
      <Face side = "z-">
        <BCType id = "0" label = "Symmetric" var = "symmetry">
        </BCType>
      </Face>
      <Face side = "z+">
        <BCType id = "0" label = "Symmetric" var = "symmetry">
        </BCType>
      </Face>
    </BoundaryConditions>
  </Grid>

</Uintah_specification>
```

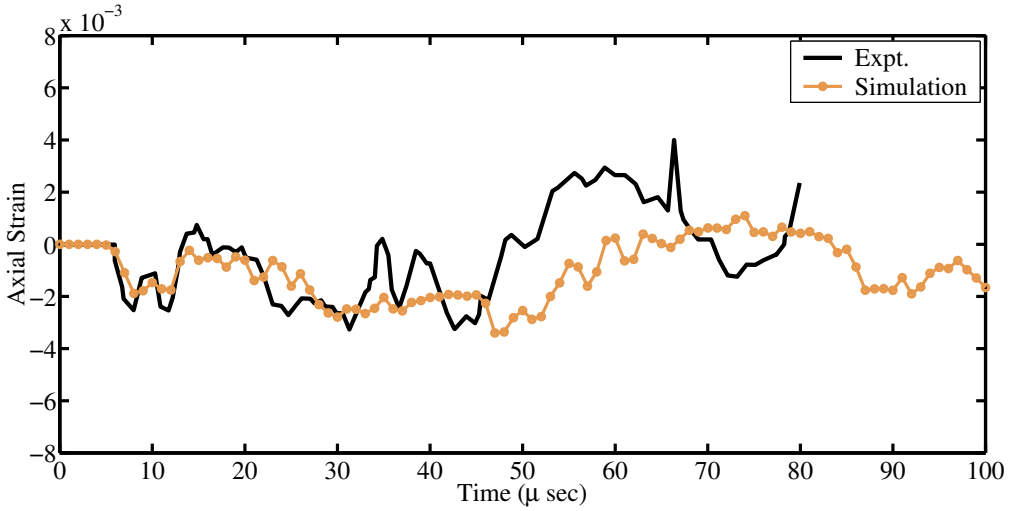

(a) Gage S1.

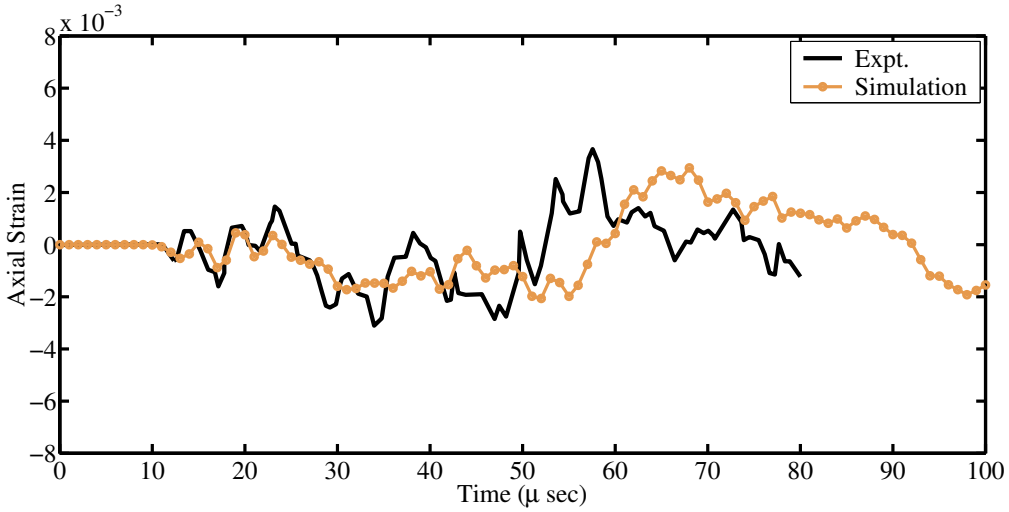

(b) Gage S2.

Figure 14: Strain histories for experiment L5: gages S1 and S2.

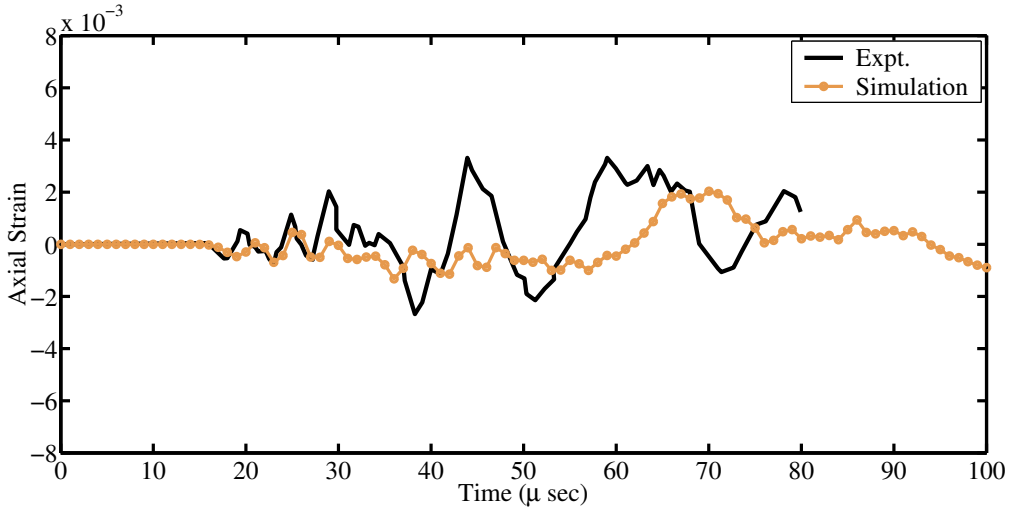

(a) Gage S3.

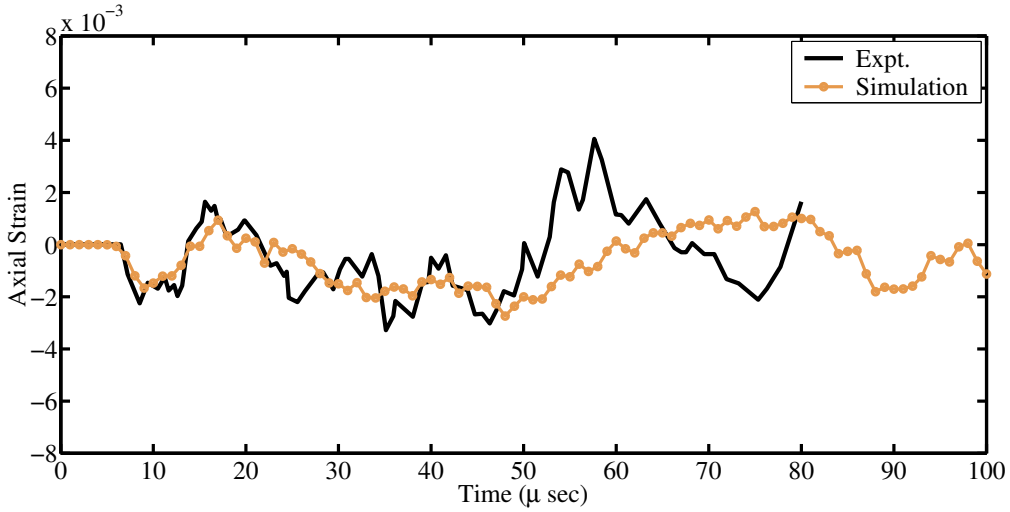

(b) Gage S4.

Figure 15: Strain histories for experiment L5: gages S3 and S4.

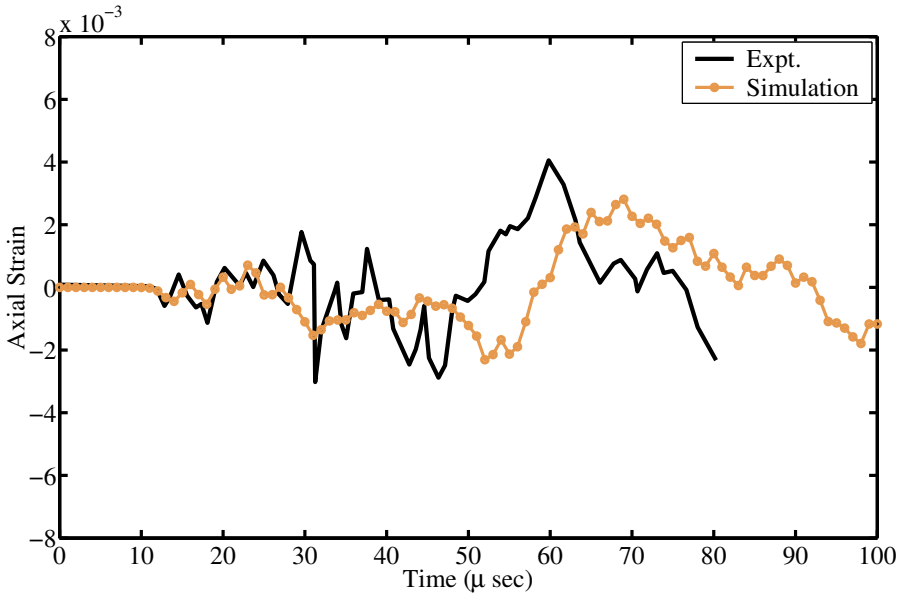

(a) Gage S5.

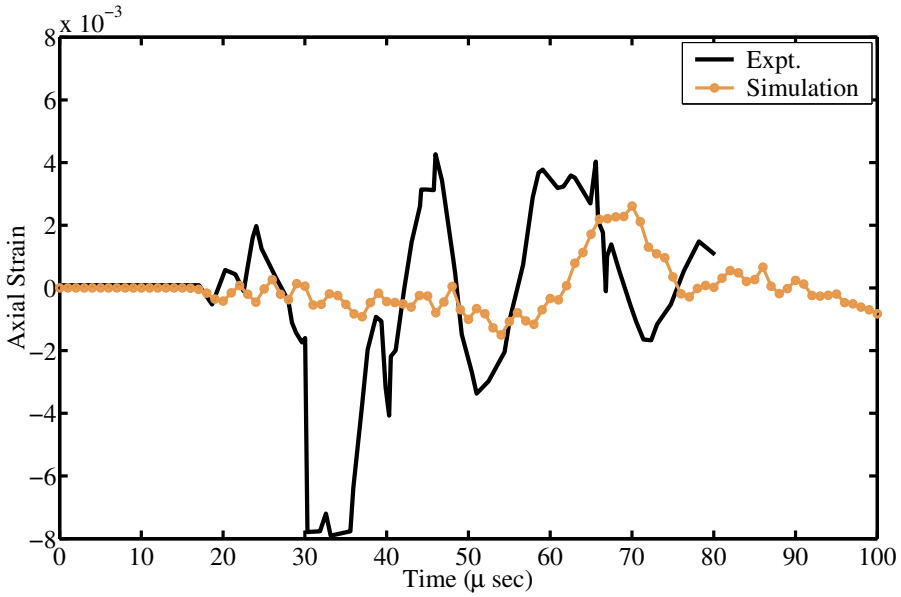

(b) Gage S6.

Figure 16: Strain histories for experiment L5: gages S5 and S6.

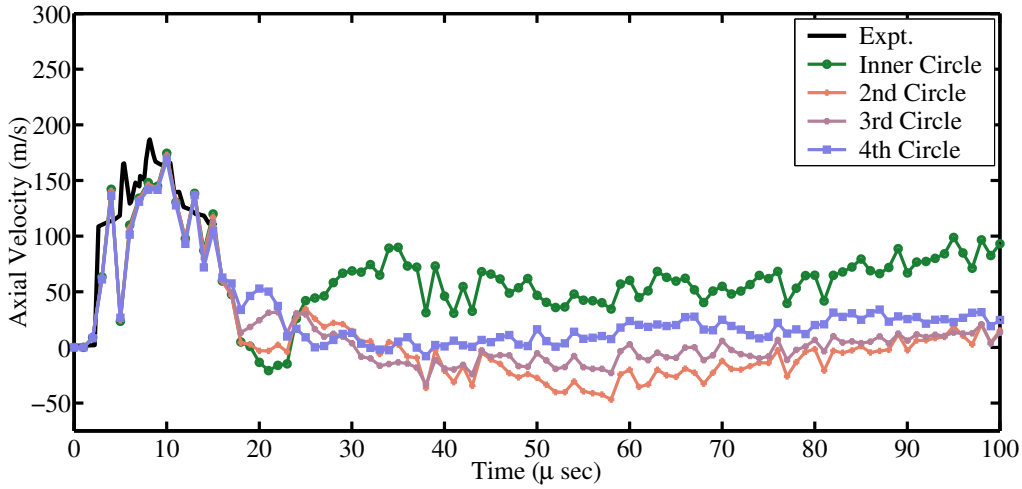

(a) Velocity history for experiment L6.

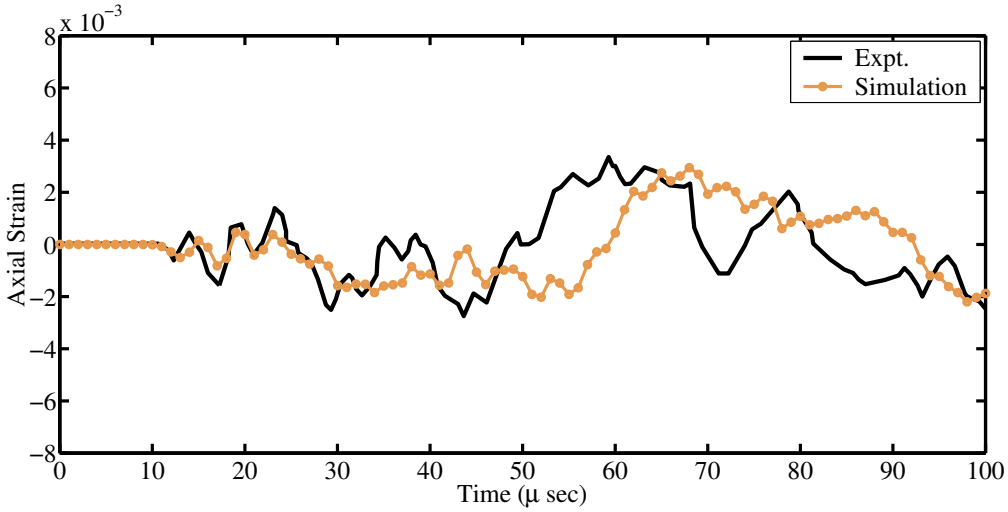

(b) Strain history for experiment L6: gage S2.

Figure 17: Velocity and axial strain history for experiment L6.